Separation and Purification Technology 305 (2023) 122396

Contents lists available at ScienceDirect

Separation and Purification Technology

journal homepage: www.elsevier.com/locate/seppur

Feasibility of several commercial membranes to recover valuable phenolic compounds from extracts of wet olive pomace through organic-solvent nanofiltration

Carmen M. Sánchez-Arévalo [a], Tim Croes [b], Bart Van der Bruggen [b], María Cinta Vincent-Vela [a,c], Silvia Álvarez-Blanco [a,c,*]

[a] Research Institute for Industrial, Radiophysical and Environmental Safety (ISIRYM), Universitat Politècnica de València, Camino de Vera, s/n, 46022 Valencia, Spain
[b] Department of Chemical Engineering (CIT), ProcESS-Process Engineering for Sustainable System, KU Leuven, Celestijnenlaan 200f - Box 2424, 3001 Leuven, Belgium
[c] Department of Chemical and Nuclear Engineering, Universitat Politècnica de València, C/Camino de Vera s/n, 46022 Valencia, Spain

ARTICLE INFO

Keywords:
Organic-solvent nanofiltration
Phenolic compounds
Sugars
Wet olive pomace
Rejection

ABSTRACT

Organic-solvent nanofiltration (OSN) has been applied to purify and fractionate the phenolic compounds present in wet olive pomace, which is the main by-product of olive mills. Nine commercial OSN membranes have been tested: DuraMem® 150, DuraMem® 300, DuraMem® 500, PuraMem® 600 (Evonik), NFS, NFX (Synder), oNF-1 and oNF-2 (Borsig) and NF270 (FilmTec). Their stability in ethanol/water 50:50 (v/v) and their effectiveness to treat a model solution of a solvent-based extract of wet olive pomace have been studied. To that end, a METcell cross-flow system (Evonik) has been utilized. DuraMem® 500, NFX and NF270 membranes displayed satisfactory values of permeate flux (10–100 $L{\cdot}h^{-1}{\cdot}m^2$) compared to the other tested membranes. Measurements of the contact angle of the membranes after their conditioning and after the nanofiltration process allowed the comprehension of the interaction between the ethanol/water 50:50 (v/v) solution and the membrane. The solvent contact angle was also examined. AFM was employed to understand the modification of membrane morphology. To characterize the samples, liquid chromatography coupled to mass spectrometry (and/or refractive index detector) was employed. The selected membranes exhibited low rejection values for the aimed phenolic compounds (less than 10 % for hydroxytyrosol) and high rejection (50–100 %) of the undesired compounds, such as sugars and organic acids. Therefore, the purification of the target phenolic compounds was accomplished.

1. Introduction

Every year, the olive oil campaign ends with the generation of enormous volumes of by-products. Depending on the methodology applied by the olive mill, there are different types of residues that can be produced. In the Mediterranean area, the three-phase methodology and the two-phase methodology are highly widespread for the production of extra virgin olive oil [1]. However, as Spain is the first world producer and the two-phase method is preferred by the olive mills from this zone, the two-phase procedure is considered to be the most common.

According to this methodology, the main residue derived from olives processing is wet olive pomace (or *alperujo*, by its name in Spanish). This by-product consists of a semi-solid combination of the olive epicarp, mesocarp and endocarp. In consequence, considerable fractions of the olive skin, pulp and stone are part of the residue. The olive fruit is rich in bioactive compounds, including phenolic compounds and vitamins [2,3]. Polyphenols are of high interest for their applications in functional foods, cosmetics and pharmacy [4]. Then, the recovery of phenolic compounds from the wet olive pomace allows the utilization of an environmentally concerning residue and the retrieval of valuable compounds that otherwise would be discarded with the by-product.

By means of an ultrasound-assisted solid–liquid extraction, it is possible to extract high concentrations of polyphenols from the wet olive pomace. It has been described previously that a mixture of ethanol/water 50:50 (v/v) can be very efficient in this context [5–7]. However, the obtained extract contains other organic compounds that are

* Corresponding author at: Research Institute for Industrial, Radiophysical and Environmental Safety (ISIRYM), Universitat Politècnica de València, Camino de Vera, s/n, 46022 Valencia, Spain.
E-mail address: sialvare@iqn.upv.es (S. Álvarez-Blanco).

https://doi.org/10.1016/j.seppur.2022.122396
Received 22 July 2022; Received in revised form 30 September 2022; Accepted 11 October 2022
Available online 17 October 2022

coextracted with the biophenols and should be then removed. The purification of the polyphenols from the hydroalcoholic extract can be achieved by membrane technology. High rejections of the organic matter have been obtained by solvent-based ultrafiltration [8,9]. However, several unwanted compounds, such as sugars and organic acids are still present in that permeate. In this context, organic-solvent nanofiltration (OSN)[1] could allow the separation of phenolic compounds from the concomitant undesired molecules present in the extract of wet olive pomace. Furthermore, OSN could be applied to perform the fractionation of the recovered polyphenols.

The growing interest of the scientific community in OSN has logically resulted in new methods for membrane synthesis. Current commercial membranes mainly include polyamide, polyimide, polysulfone, polydimethylsiloxane, polybenzimidazole and polyacrylonitrile as a polymer. Moreover, the development of novel materials that improve OSN procedures has become very relevant [10,11]. In the recent years, carbon organic frameworks (COFs) and metal–organic frameworks (MOFs) have emerged as porous materials with tunable pore size and high chemical resistance, which opens a new range of opportunities regarding molecular separations [12–14]. In fact, membrane preparation is the main topic of the research in this membrane technology field [15].

However, thoughtful and further research about the real application of the recent solvent-resistant polymers that are being produced and commercialized is needed. The latter has been more common regarding aqueous nanofiltration [1,16–18], but it is still a growing area when it comes to OSN.

In this contribution, several OSN membranes, as well as conventional ones, have been tested to study their stability and performance regarding the purification and fractionation of the phenolic compounds present in the wet olive pomace. For that purpose, a model solution of a hydroalcoholic extract of wet olive pomace has been employed. Its pretreatment by ultrafiltration has also been considered when preparing the simulated solution. The rejection of undesired compounds was not the only objective. The separation of the polyphenols of interest was also pursued, in order to obtain them in fractions of individual or very similar molecules, which will enhance their potential industrial application.

Among the membranes tested in this study, a wide range of pore sizes was contemplated, including membranes with reduced values of molecular weight cut-off (MWCO), such as the NFS membrane (100–250 Da), and also loose nanofiltration membranes with larger pores, as the oNF-1 membrane (600 Da). Additionally, several manufacturers were considered, namely FilmTec, Evonik, Synder and GMT-Borsig, in order to study a diverse repertoire of the current commercial catalog. Most of them are acknowledged producers of OSN membranes. Then, the selection of different commercially available membranes, resistant to ethanol/water 50:50 (v/v) (which is the working solvent in this work) and provided by the main OSN manufacturers was intended. Additionally, the NF270 membrane, which is a conventional membrane (not specifically designed to work with organic solvents) was included in the study. This membrane is extensively employed in the literature, and it has proven to be effective for the recovery of valuable compounds from agro-food samples. The separation of phenolic compounds and sugars in an aqueous medium has already been described with this membrane [17]. Then, its performance in a hydroalcoholic environment was considered of interest.

[1] Abbreviations: AFM: atomic force microscopy; COF: carbon organic framework; DAD: diode-array detector; LC-MS: liquid chromatography coupled to mass spectrometry; MOF: metal–organic frameworks; MWCO: molecular weight cut off; OSN: organic-solvent nanofiltration; PDMS: polydimethylsiloxane; QToF: quadrupole-time-of-flight; TIC: total ion chromatogram; TMP: transmembrane pressure; VRF: volume reduction factor.

2. Materials and methods

2.1. Solvents and reagents

Pure ethanol and LC-MS grade acetonitrile were purchased from VWR (USA); extra-pure sulfuric acid, LC-MS grade formic acid and LC-MS grade acetic acid were obtained from Fisher (Fisher Scientific, USA). Ultrapure water was obtained from an Arium® system (Sartorius, Germany). The pure standards of phenolic compounds and triterpenic and fatty acids were purchased from VWR (in the case of tyrosol, luteolin, caffeic acid and citric acid) and Sigma Aldrich (USA) in the case of hydroxytyrosol, oleuropein, decarboxymethyl-oleuropein aglycone, *p*-coumaric acid and hydroxy-stearic acid. Sigma Aldrich also provided the standards for sucrose, D-glucose, and D-fructose.

2.2. Feed solution

A model solution of the permeate obtained in the ultrafiltration of a hydroalcoholic extract of wet olive pomace was prepared. This model solution corresponded to the permeate obtained in an XFUF 076 01 bench-top ultrafiltration cell (Merck Millipore, USA) with the UP005 membrane (Microdyn Nadir, Germany) at 2 bar. This permeate was analyzed as detailed in Section 2.5.1. The determined concentrations of each chemical class present in the ultrafiltration permeate can be revised in Table 1.

The analysis through liquid chromatography coupled to mass spectrometry (LC-MS) allowed the determination of seven chemical families, including simple phenols, secoiridoids, flavonoids, phenolic acids (all of them being phenolic compounds), triterpenic acids, and free fatty acids. Sugars were also detected by global analysis (Section 2.5.1). To simulate this content, not only one compound was included, but all the chemical families present in the real stream. Thus, at least one representative for all the chemical classes of the ultrafiltered extract of wet olive pomace was added to the solution. To select one compound as a family representative, the most concentrated one was chosen. When the most concentrated molecule of one chemical class was not commercially available, then the following compound in abundance was selected.

The concentration of the analytes was set according to the actual concentrations present in the real sample. The representative of each chemical family was added at the total concentration of the entire chemical class. For example, the representative for the class of flavonoids (luteolin, in this case) was added at 15 ppm, because this was the sum of concentrations of all the flavonoids present in the sample. Logically, the total concentration of each family was not an exact number. Thus, the concentration value was rounded to the most proximate multiple of 5, in order to facilitate the preparation of samples. Two compounds from the same family were added to the solution in some cases. This occurred when both of them were of high importance because of their chemical structure or economic implications. Then, their relative concentration in the real stream was maintained in the solution. The selection of the representative compounds was made according to their presence in the real sample, their industrial and scientific relevance, and their commercial availability.

In the case of sugars, the ripening stage of the olive fruits (as a prime matter for the generation of wet olive pomace) was taken into account. The extract of wet olive pomace would contain a different concentration of soluble sugars depending on the moment of the olives' harvesting and the time between their harvesting and their processing. As the olive ripening occurs, the polysaccharides from the vegetal cell (including cellulose and hemicellulose, among others) suffer a degradation that results in the release of some of their monomers, increasing the concentration of soluble sugars [19,20]. Then, to better simulate the sugar content of the ultrafiltered hydroalcoholic extract of wet olive pomace, a higher concentration of soluble sugars was contemplated, although the relative concentration of glucose, fructose and sucrose [21] was maintained. The detailed composition of the model solution is shown in

Table 1
Composition of the model solution employed as feed for the organic solvent nanofiltration process.

Compound	Molecular weight (g/mol)	Concentration in *alperujo* UF Permeate (ppm)[a]	Chemical Family	Total concentration of the chemical family (ppm)	Concentration in the model solution (ppm)	Justification
Tyrosol	138.2	0.728	Simple phenols	49.403	25	Both of them are key representatives of simple phenols. Hydroxytyrosol is extremely valued by industry.
Hydroxytyrosol	154.2	45.113			25	
Oleuropein	540.5	0.950	Secoiridoids	958.549	150	Main representative of secoiridoids in literature. High industrial relevance.
Decarboxymethyl oleuropein aglycone	320.3	8.040			10	As a representative of secoiridoids.
Luteolin	286.2	10.570	Flavonoids	14.411	15	As a representative of flavonoids.
Caffeic acid	180.2	115.304	Phenolic acids	122.045	120	As a representative of phenolic acids.
p-Coumaric acid	164.1	3.317			5	As a representative of phenolic acids. High industrial relevance.
Hydroxy-stearic acid	300.5	1.400	Free fatty acids	3.543	5	Free fatty acids are present in the real sample and hinder the purification of polyphenols.
Citric acid	191.1	310.820	Organic acids	326.973	350	Organic acids hinder the purification of polyphenols from the sample.
Sucrose	342.3	300	Sugars	300	50	Sugars hinder the purification of polyphenols from the sample.
Fructose	180.2				300	
Glucose	180.2				1500	

[a] UF Permeate obtained with membrane UP005, at 2 bar.oNF-2,/350.

Table 1. Information about the molecular weight, concentration in the real sample, and concentration in the model solution are displayed. Additionally, the Table shows the chemical class that is represented by these compounds, its total concentration, and the justification of the representative selection.

The three-dimension structure of the analytes present in the feed solution was analyzed with the software Jmol, which is an open-source Java viewer for chemical structures in 3D (https://www.jmol.org). This software also allowed the calculation of the distance between each atom of the molecules.

2.3. Organic solvent nanofiltration set-up and experimental procedure

All experiments were carried out in a *METcell* Cross-Flow System (Evonik Industries, Germany), with two membrane modules set in series. The effective area of each module was 14.6 cm^2. In total, 9 commercially available, organic membranes, of which the specifications can be found in Table 2, were tested.

A new membrane coupon was employed for each experiment. Prior to their utilization, the membranes were immersed in ethanol/water 50:50 (v/v) for at least 12 h, in order to precondition them. Moreover, a compaction stage was carried out before running any experiment. Thus, the permeate flux, $J_p(L{\cdot}h^{-1}{\cdot}m^{-2})$, was monitored until a stable permeate flux was observed, at a transmembrane pressure (TMP) of 38 bar, or 20 bar, in the case of the Dm500 membrane. Apart from the obtention of a compacted separation layer for the membranes, their stability in the presence of the organic solvent was tested. A stable permeate flux during that time determined that the polymer was not damaged by the solvent and, furthermore, it confirmed the removal of any remaining preservative agent. To characterize the membranes, the solvent permeability was calculated according to the equation:

$$L_p = \frac{J_p}{TMP} \quad (1)$$

Afterwards, the synthetic feed solution was nanofiltered at 36 bar (or 20 bar, in the case of the Dm500 membrane). The permeate flux was monitored and permeate samples were taken at a volume reduction factor (VRF) of 3 for their analysis. When some membranes were considered best in terms of performance, they were further investigated at other values of TMP (15 and 25 bar) and the rejection was evaluated at different values of VRF. The experiments were carried out in duplicates, with a maximum relative standard deviation of 13.5 % (intra-day repeatability).

The morphology of the active layer of each membrane was studied before and after their immersion in the solvent. To that end, atomic force microscopy (AFM) was employed, using a MultiMode 8 AFM instrument (Bruker, Germany), equipped with a ScanAsyst-Air probe (Bruker, Germany). The working methodology was Quantitative Nanomechanical Mapping. The obtained images were processed with the software NanoScope Analysis 1.8.

The cleaning of the most promising membrane was also studied. After its utilization, the NF270 membrane was conveniently cleaned with an Ultrasil 1 % (v/v) solution. The recovery of the initial solvent permeability of the membrane surpassed 98 %. Then, the membrane could be recycled in subsequent experiments.

Table 2
Specifications of the membranes employed in this work. The data have been retrieved from the manufacturers.

Membrane	MWCO[a] (Da)	Material	Manufacturer	Maximum operating pressure (bar)
NF270	300–400	Polyamide	FilmTec	41
Dm150[b]	150	P84® polyimide	Evonik	60
Dm300[c]	300			
Dm500[d]	500			20
Pm600[e]	600	Silicone-coated polyimide		60
NFS	100–250	Proprietary polyamide	Synder	41
NFX	150–300			
oNF-1	600	Polydimethylsiloxane	GMT-Borsig	40

[a] MWCO: molecular weight cut off.
[b] Dm150: DuraMem®150.
[c] Dm300: DuraMem®300.
[d] Dm500: DuraMem®500.
[e] Pm600: PuraMem®600.

2.4. Adsorption

To evaluate the adsorption of phenolic compounds on the membrane surface, an HP4750 dead-end filtration cell (Sterlitech, USA) was used. The olive–pomace model solution was placed in the cell to be in contact with the membrane surface for 24 h, in agitation mode. No pressure was applied. The membranes were previously preconditioned as explained in Section 2.3, in order to obtain adsorption results comparable to those

occurring during the nanofiltration process. All experiments were carried out in duplicate.

The concentration of the compounds in the solution before and after this period was compared and used to calculate the adsorption, as in the following formula:

$$Q = \frac{C_0 - C_f}{A} \cdot V \quad (2)$$

where Q represents the mass of the adsorbed compound per membrane surface unit ($mg \cdot m^{-2}$), C_0 ($mg \cdot L^{-1}$) is the initial concentration of the compound in the solution, C_f ($mg \cdot L^{-1}$) is the final concentration of the compound after the adsorption test, A (m^2) is the membrane area and V (L) is the volume of the solution employed during the experiment.

This methodology was developed by Arsuaga and co-workers [22,23] and has been later reproduced [24].

2.5. Sample characterization

2.5.1. Analysis of ultrafiltration permeate to establish the composition of the model solution

The individual composition of the ultrafiltration permeate, intended to be the feed for the nanofiltration process of this work, was determined by LC-MS. The applied methodology was developed in an earlier work [25], using a 1260 Infinity II LC system coupled to a quadrupole-time-of-flight (QToF) mass spectrometer (Agilent Technologies, USA). Shortly, a Zorbax Extend C18 column (4.6 × 100 mm, 1.8 μm) (Agilent Technologies, USA) was employed for the separation of the compounds, operating at 40°C. Injection volume was 4 μL. Analytes elution was conducted with a gradient of acetonitrile and water, both acidified with a 0.5 % acetic acid, and a flow rate of 0.8 m/min. Acquisition of MS data was performed in negative ionization mode.

Total soluble sugars were analyzed by the Anthrone methodology [26,27].

2.5.2. Characterization of the organic solvent nanofiltration streams

2.5.2.1. Analysis of phenolic compounds and triterpenic and free fatty acids. To characterize the OSN streams, compounds were individually determined by means of a 1100 Agilent liquid chromatograph coupled to a 6110 single-quadrupole (Agilent Technologies, USA). After a 5 μL injection, analytes were eluted throughout the column mentioned in Section 2.5.1, at a flow rate of 0.5 mL/min. To that end, the following gradient was applied: 5 % B at initial conditions, 20 % B at 1 min, 85 % B at 7 min, 100 % B at 7.5 min, where water acidified with a 0.5 % of formic acid was the solution A and acetonitrile was the solution B. 100 % of solution B was maintained until minute 10 and then the gradient went back to the initial conditions. The MS acquisition was set in negative ion mode and single ion monitoring, with the [M−H] value of *m/z* of each compound. All samples were injected at least twice.

Data analysis was performed with the software ChemStation B.04.02 (Agilent Technologies, USA). All compounds were quantified by integrating the peaks obtained in the base peak chromatogram provided by the mass spectrometer. Only the peak of tyrosol was integrated through the diode-array (DAD) signal (also provided by the instrument), because the DAD signal for this compound was considered to be more reliable, considering the injection solution and the applied gradient.

Solutions of pure standards were prepared in ethanol/water 50:50 (v/v), in the range 0.1–100 ppm, and used for the external calibration.

2.5.2.2. Determination of sugars. Sucrose, glucose, and fructose concentrations were determined by an Agilent 1200 liquid chromatograph coupled to a refractive index detector (Agilent Technologies, USA). The instrument was equipped with the column Aminex HPX-87H (Bio-rad, Belgium), kept at 40°C during the analysis and protected with a Micro-Guard cation H guard column (Bio-rad, Belgium). 5 mM sulfuric acid was used as a mobile phase, at a flow rate of 0.6 mL/min. The injection volume was 20 μL. All vials were injected in duplicates. For data processing, ChemStation B.04.02 was employed.

2.6. Contact angle measurements

To assess the hydrophilic or hydrophobic character of the membranes surface, a contact angle analyzer Krüss DSA10 Mk2 (Krüss Optronics, Germany) was employed. Water droplets of 20 μL were gently delivered on the membrane surface by a microsyringe. Then images of the drop were taken during 3 s and the contact angle was measured. This process was repeated 10 times on different sections of the membrane surface, and the mean values have been reported.

3. Results

3.1. Synthetic ultrafiltration permeate of wet olive pomace

The composition of the feed solution (Table 1) was carefully designed to include all the chemical families present in the permeate resulting from the ultrafiltration of an extract from wet olive pomace obtained with ethanol/water 50:50. In the ultrafiltration step, a high proportion of organic matter was already removed. However, some unwanted species were still present in the permeate stream. Therefore, it is key to consider these compounds too, in order to evaluate the effectiveness of the OSN to purify the phenolic compounds. Among these concomitant, undesired molecules, there are sugars (including sucrose, glucose and fructose), organic acids (represented by citric acid in this feed solution) and free fatty acids (represented by hydroxy-stearic acid). Regarding the biophenols, compounds from all the chemical classes present in the real sample were added to the solution. This aspect is important, since the different phenolic families differ in size, chemical structure and polarity, and this may lead to different solute-membrane interactions, as demonstrated in the literature for different solvents, solutes and membrane materials [10,22,28].

Fig. 1 shows a chromatogram obtained after the analysis of the feed solution by LC-MS (as detailed in Section 2.5.2.1).

As can be seen, the composition of the feed solution covers a wide range of chemical structures. These compounds were at high concentration in the sample that has been simulated. In consequence, the content of the simulated wet olive pomace extract was considered to properly reproduce the characteristics of the original sample. The pH of the model solution was 4.4 ± 0.3, which also was in accordance with the real stream, which had a pH of 5.2 ± 0.3.

To better assess the size and atoms distribution of the compounds from the simulated wet olive pomace solution, their three-dimension molecular structure and the distance between the atoms have been presented in Fig. 2.

As shown in Fig. 2, citric acid is the smallest compound in the solution. It has a non-linear conformation, with several polar end-groups, such as –CO and –OH. Regarding the phenolic compounds, the characteristic benzenic ring can be observed in all molecules. The distance between the carbon atoms of this benzenic structure is 0.28 nm. Several functional groups and side chains can be bonded to the benzene in the different molecules, and the position, number and length of these radicals determine the identity of the compound, its polarity and its molecular width. Therefore, the rejection during the nanofiltration process will be affected too. Among the phenolic compounds, two groups can be differentiated. On one side, tyrosol, hydroxytyrosol, caffeic acid and *p*-coumaric acid only contain one phenolic ring. Their structure differs in the number of hydroxyl radicals (the distance between a carbon from the phenol ring and a bonded oxygen is 0.14 nm) and the composition of the side chain, which influences the molecular length.

On the other side, the molecules of luteolin, decarboxymethyl oleuropein aglycone and oleuropein contain more than one ring in their structure. As shown in Fig. 2, this determines a larger, more ramified

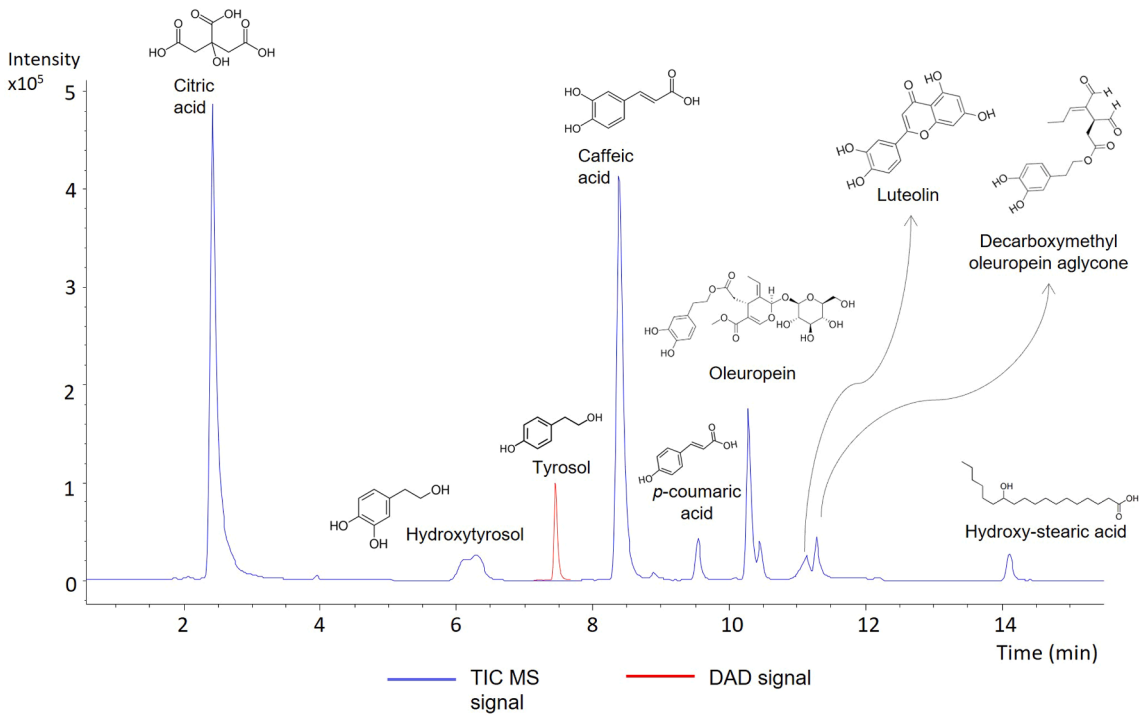

Fig. 1. Total ion chromatogram (TIC) of the simulated wet olive pomace extract. All compounds were determined by liquid chromatography coupled to mass spectrometry, except for tyrosol, which was detected by means of a diode-array (DAD) detector. The absolute scale for that compound is not shown in the figure.

structure in comparison to the previously cited compounds. Finally, hydroxy-stearic acid is a linear fatty acid with a distance of 2.24 nm between the first and the last carbon of the chain. The relative disposition of this molecule in the surrounding of the membrane pores will influence its rejection.

3.2. Evaluation of the permeate flux

Fig. 3 shows the permeate flux obtained at 36 bar (20 bar in the case of Dm500) with the different membranes tested. The permeate flux obtained when the pure solvent and the model solution were nanofiltered can be observed. Logically, flux values were lower in the case of the model solution.

According to the figure (Fig. 3), three groups can be differentiated regarding the permeate flux of ethanol/water 50:50 (v/v) and the model solution. The lowest fluxes were obtained with the membranes Dm150, Dm300, and Dm500. The solvent permeability of the Dm150 membrane was 0.15 $L{\cdot}h^{-1}{\cdot}m^{-2}{\cdot}bar^{-1}$. Thus, this membrane was not considered for the nanofiltration of the synthetic extract of wet pomace, because the solvent flux was already not sufficient. Low differences were found between the solvent permeability of Dm300 (0.70 $L{\cdot}h^{-1}{\cdot}m^{-2}{\cdot}bar^{-1}$) and Dm500 (0.95 $L{\cdot}h^{-1}{\cdot}m^{-2}{\cdot}bar^{-1}$) membranes, even though their MWCO is not similar. Considering the higher MWCO of the Dm500 membrane and its thinner active layer, a higher permeability was expected. However, this was not observed. A similar phenomenon was reported by Peshev et al. [29], who obtained lower values of permeate flux for the Dm500 membrane (with respect to the Dm300 membrane) during the nanofiltration of a solution of caffeic and rosmarinic acid in ethanol. Also, Tylkowski and co-workers [30] observed a similar permeate flux for both membranes. These authors determined by scanning electron microscopy that these two membranes presented a different structure. According to them, the active layer of the Dm300 membrane is denser, whereas the Dm500 membrane displays a finger-like structure. Due to the different structure, these authors observed that the thickness of the active layer of the Dm300 membrane remained unchanged after filtration at 50 bar, while it showed a decrease of about 31 % in the case of the Dm500 due to compaction. These authors attributed the unexpected, low permeability of the Dm500 membrane to the compaction of the active layer at high pressure, which was not observed for the Dm300.

The NFS and NFX membranes can also be paired in the discussion, because both reported similar values of permeate flux and solvent permeability (1.2 $L{\cdot}h^{-1}{\cdot}m^{-2}{\cdot}bar^{-1}$ for NFS and 1.1 $L{\cdot}h^{-1}{\cdot}m^{-2}{\cdot}bar^{-1}$ for NFX). However, the highest jump in permeate flux was featured by the NF270 membrane (with a solvent permeability of 3.3 $L{\cdot}h^{-1}{\cdot}m^{-2}{\cdot}bar^{-1}$). This high flux could be due to the high hydrophilicity of the membrane material (see Table 4). The NFX membrane was also highly hydrophilic, but its lower MWCO led to a lower permeate flux. Also, both the NFX and the NF270 membranes are composed of polyamide, however, the manufacturer of the NFX membrane reports the material as “proprietary polyamide”, which suggests the implementation of modifications to the polymer. This can explain the lower flux, along with the smaller pore size.

Considering the outstanding values of permeate flux obtained with the NF270 membrane and the interesting rejection values that will be exposed in Section 3.3, this membrane was further investigated at the TMPs of 15 and 25 bar (Fig. 3) to treat the simulated extract of wet olive pomace.

An increment in the permeate flux with TMP was observed, which indicated that no significant membrane fouling occurred. In view of the outstanding values of permeate flux obtained at 36 bar, these nanofiltration tests were conducted until higher VRF values were achieved. This also permitted to explore the rejection at a larger concentration level.

Regarding the membranes from GMT-Borsig, no permeation at all was obtained when treating the pure solvent, at any pressure in a range of 8–40 bar. This was observed for the oNF-2 membrane, but also for the oNF-1 membrane, in spite of having a very high MWCO (600 Da). No further pressure could be applied, as the manufacturer reported 40 bar as the maximum permitted pressure for this membrane (see Table 2). According to [31], the contact angle value of the membrane oNF-2 was 87°, which can be related to a low polarity. Therefore, considering the composition of the working solvent, the solvent-membrane interaction

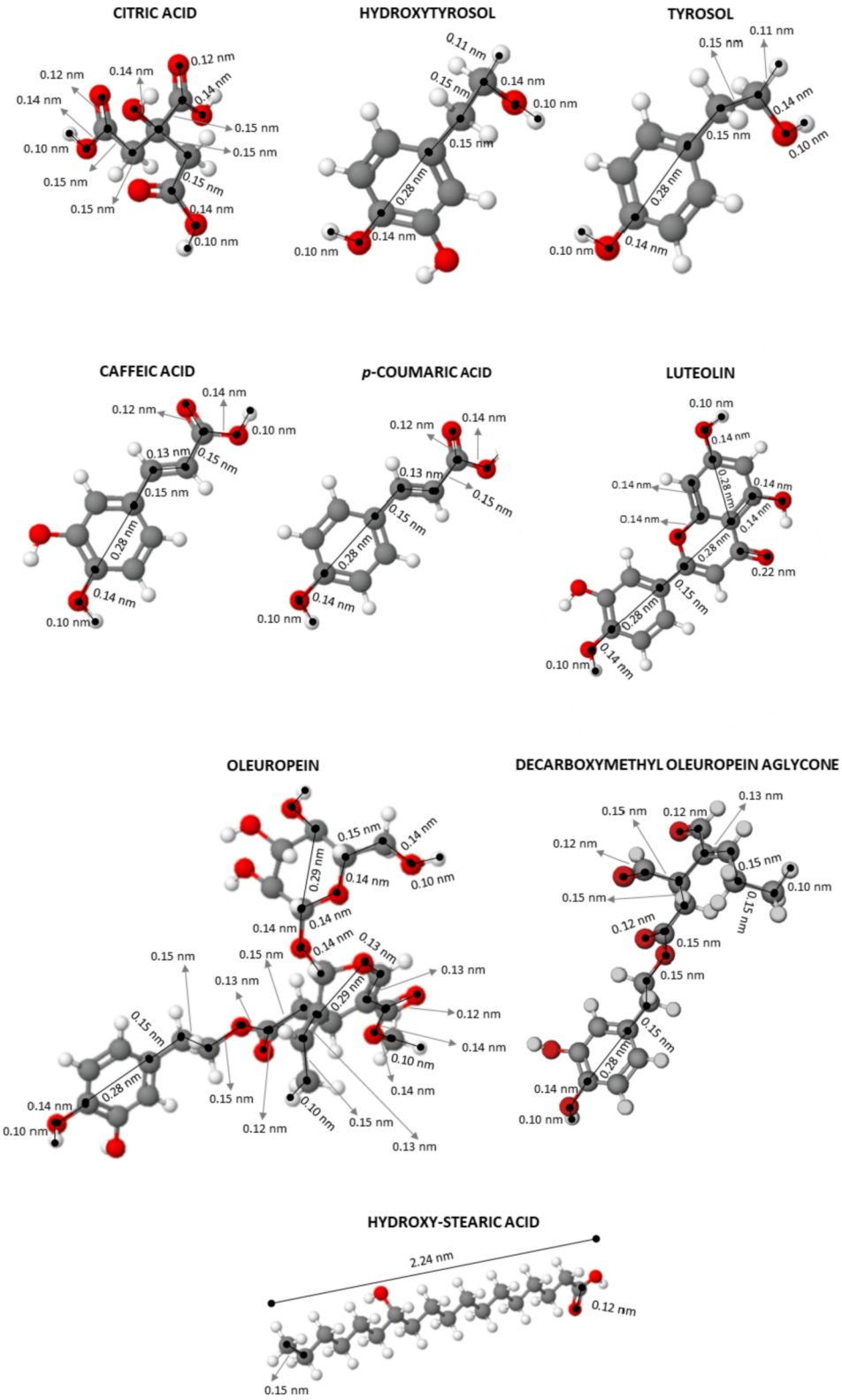

Fig. 2. Three-dimension structure of the compounds present in the simulated solution of wet olive pomace. The distance between the atoms has also been provided. Oxygen has been presented in red color, carbon corresponds to grey color and hydrogen has been presented in white color. (For interpretation of the references to color in this figure legend, the reader is referred to the web version of this article.)

was not favored. In fact, the solvent was unable to wet the polymers and formed drops that later slipped off the membrane surface, as can be seen in Supplementary Fig. 1. Previously reported results [28,32] showed that the permeability to ethanol was very low for this membrane (near 0.15 $L{\cdot}h^{-1}{\cdot}m^{-2}{\cdot}bar^{-1}$), while water permeability was zero. These authors related the solvent permeability to the difference between the solubility parameter of the polydimethylsiloxane (PDMS) polymer and that of the solvent, being greater if the difference is small and extremely low or even zero if the difference is large [28,32].

Similarly, the Pm600 membrane produced no permeate at all,

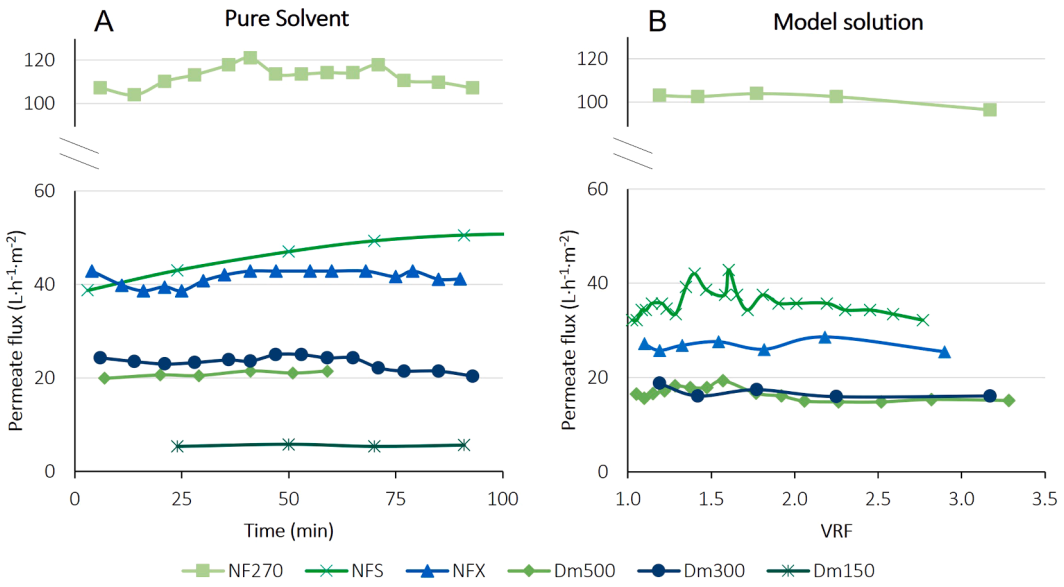

Fig. 3. Values of permeate flux obtained with the membranes tested. Panel A shows the results for the pure solvent (ethanol/water 50:50 (v/v)) and panel B refers to the wet olive pomace extract model solution. Nanofiltration was carried out at 36 bar for all membranes except for DuraMem®500 (20 bar).

irrespective of the applied pressure. According to the manufacturer, the membrane material is silicone-coated polyimide. Silicones are highly hydrophobic materials. The contact angle of silicones has been reported to be greater than 100° [33], while the solvent (ethanol/water 50:50 (v/v)) is highly polar. Then, the same as in the case of GMT-Borsig membranes, the solvent was not able to wet the Pm600 membrane, as can be observed in the supplementary information, where it can be appreciated (Supplementary Fig. 1) that the membrane repelled the solvent. The manufacturer recommends using the membrane in non-polar solvents. As a consequence, the oNF-1, oNF-2 and Pm600 membranes were not employed during the nanofiltration of the wet olive pomace solution.

3.3. Fractionation of phenolic compounds

The objective of the nanofiltration process that has been developed here is to enhance the purity of the polyphenols. Apart from sugars rejection (which will be commented in Section 3.5), the separation of the phenolic compounds from other organic molecules is relevant. In this case, citric acid and hydroxy-stearic acid were present in the feed solution as undesired compounds. As can be observed from Fig. 5, most of the membranes performed satisfactorily in terms of rejection values. All of them rejected the free fatty acid (hydroxy-stearic acid) almost completely (Fig. 5). Citric acid was better rejected by the Dm300, Dm500 and NFX membranes, even though the molecular weight of this compound (192 g/mol) was below the MWCO of all the membranes.

Several authors have discussed that the molecular weight of a compound is not sufficient to understand other properties such as hydrogen bonding capacity, hydrophilicity, etc. In fact, it is not rare to find in the literature rejection values of 100 % for compounds that should permeate if only their molecular weight is considered. For example, Peshev et al. found rejection values of 82–97.4 % for phenolic acids around 180 g/mol after an ethanolic OSN process with the membranes DuraMem® 300 (MWCO of 300 Da) and DuraMem® 500 (MWCO of 500 Da) [29]. Vieira and co-workers also found that cyanidin-3-glucoside and cyanidin-3-rutinoside, which were below the MWCO of the NP010 membrane, exhibited a rejection larger than 50 % [34]. This is another indicative of many other characteristics of the molecules being relevant in their rejection. Ignacz and Szekely measured the rejection values of 336 different molecules using three commercial DuraMem® polyimide membranes with different MWCO values in methanol [35]. They demonstrated that the chemical structure of the compounds affected solute rejection. For instance, they related the presence of carboxylic groups to substantially increased values of rejection, and citric acid presents three carboxylic groups. Thus, functional groups, atoms disposition and chemical structure of the compounds may also influence this phenomenon [28,35]. These authors also observed that rejection was more dependent on the molecular weight if the solvent presents a higher affinity towards the membrane [35]. As commented in Section 3.1, the presence of different radicals and electronegative atoms in the molecule will determine its charge and polarity, influencing the affinity between a compound and the membrane. Moreover, the relative conformation of the atoms within the molecule can determine its shape, which is also very relevant when it comes to its transport throughout the membrane pores.

Only the NFS membrane was unable to reject citric acid. To the best of our knowledge, this is the first time that the NFS membrane has been tested in this context. Its performance has only been reported twice in the literature, through the study of its surface modification [36] and the treatment of industrial wastewaters [37]. Table 4 indicates that the NFS membrane had an initial contact angle of 49.79° [36] and it changed to 26 ± 2° after its preconditioning. This variation corresponds to the relative orientation of the ethanol molecules on the membrane surface. In comparison with this membrane, the NFX displayed a similar contact angle (with respect to NFS) after its immersion in ethanol at 50 % (v/v) and the NFX membrane did reject citric acid (72.7 ± 10.7 %). However, the contact angle of the NFX membrane increased after the conditioning. This indicated that the reorganization of the membrane surface structure after the overnight immersion in ethanol/water 50:50 (v/v) could have occurred differently for these two membranes. Van der Bruggen and co-workers already reported that a modification of the membrane structure can alter its polarity [38]. Considering the chemical structure of the ethanol molecules present in the solution, it can be inferred that the more polar hydroxyl radical would be oriented to the feed side, whereas the rest of the molecule (with a lower relative polarity) would preferentially interact with the pore walls of the NFS membrane, because of a higher affinity between the membrane and the more hydrophobic carbon tail. This effect led to a greater exposition of polar groups towards the bulk solution, increasing the hydrophilicity of the active layer. In the case of the NFX membrane, the opposed orientation of the ethanol molecules could be suggested. This effect has been observed before [39–41] for different membrane materials and solvents and could explain the modulation of the membrane contact angle, which was

reduced almost by half for the NFS membrane. For instance, de Melo et al. observed that hexane flux through ceramic membranes, which are highly hydrophilic, increased to a large extent after pre-treatment with *n*-butanol. They attributed the flux enhancement to the interaction of the polar head with the polar pore surface of the membrane and the non-polar tail would then be oriented to the bulk solution [39]. These interactions would also explain the higher permeate flux observed for the NFS membrane in comparison with the NFX despite of having lower MWCO. In such a scenario, the affinity between the citric acid and the rearranged NFS membrane surface (with more hydroxyl groups available to interact with the solute) could have been increased, leading to a higher passage. However, the opposed orientation of the ethanol molecules in the case of the NFX membrane did not favor the permeation of citric acid.

In addition to the polarity, the presence of several electronegative atoms in the structure of citric acid (Fig. 2) suggests the interaction with the NFS membrane, considering its low water contact angle. Additionally, some electrostatic interactions can be also considered. This is the compound in the feed solution with the lowest pK_a, corresponding to 2.79. Being the pH of the model solution around 4.4, it is reasonable to accept that the molecule of citric acid was negatively charged. The pK_a of the rest of the compounds is above 4, indicating that the molecules are neutral. Regarding the membranes, most of them exhibit an isoelectric point close to the pH of the feed solution. The isoelectric point of the NF270 membrane has been reported to be between 3 and 5.2 [42,43]. The Dm300 and Dm500 membranes have an isoelectric point of 4.8 [44] and for the NFX and NFS membranes, this value is 3.2 and 3.8, respectively [36,45]. According to these values, only the NF270 and NFX are expected to be (at least partially) negatively charged. Then, an electrostatic repulsion can be related to the high rejection of citric acid observed with the NFX membrane in comparison with the NFS membrane, despite a similar contact angle between both membranes.

Finally, the chemical structure of citric acid may have also influenced its rejection. As mentioned, other characteristics of the molecules apart from the molecular weight (such as the size of the compound or the molecular width) are better related with steric interaction between the compound and the membrane pores [46]. Being NFS the tighter membrane tested here and citric acid the smallest and more polar molecule from the feed solution, the obtained rejection values were considered to be acceptable. These results suggest the possibility of applying this membrane to remove citric acid (which could even be recovered from the permeate, if desired) and obtain a retentate enriched in phenolic compounds. Considering the chemical structure of this molecule, it could be concluded that other organic acids that also occur in olive-derived wastes at high concentrations [25], such as malic acid and quinic acid, could be removed too by means of this membrane.

The Dm300 membrane rejected the compounds of high molecular weight. Among the smaller molecules, a marked specificity for caffeic acid was observed, despite what could be expected due to its molecular weight. In comparison with the molecules of hydroxytyrosol and tyrosol, this compound can be considered relatively less polar, because it contains an additional atom of carbon in the side chain and, furthermore, its elution from a C18 non-polar column takes place later (see Fig. 1). According to different authors, the permeation trough the Dm300 membrane is highly dependent on the physicochemical solute properties causing interactions with both membrane and solvent [30,35]. Thiermeyer et al. concluded that solute transport through this membrane is affected by the affinity between the solute and the membrane [47]. They demonstrated that, in polar solvents such as ethanol and isopropanol, polar solutes showed a tendency to higher rejections than moderately polar solutes. Therefore, considering these results, the less polar character of the caffeic acid favored its permeation through the membrane.

Fig. 5 clearly shows that the largest compounds did not pass any of the membranes, because luteolin, decarboxymethyl oleuropein aglycone and oleuropein were always rejected in high percentages. These results allowed the fractionation of the polyphenols according to their molecular weight, which was also one of the objectives of this work. In most of the cases, small-size phenolic compounds (in the range of 138–180 g/mol), which were below the MWCO of the membranes, were recovered in the permeate. This trend was very marked for the Dm500 membrane, which allowed the purification of hydroxytyrosol, tyrosol, caffeic acid and *p*-coumaric acid, all of them considered very valuable compounds [48,49]. In contrast, Peshev et al. found high rejections of caffeic acid when these membranes were used to nanofilter a rosemary extract [29]. Nevertheless, those extracts were prepared in pure ethanol, and the membrane conditioning was conducted with this solvent too. On the other hand, caffeic acid concentration was significantly smaller than the one considered in our work and their tests were performed at constant volume operating mode, by recirculation of the permeate to the feed tank. The duration of their tests was also much shorter than in this work. According to several authors [50–52], solute adsorption has a relevant role in nanofiltration rejection. As a result, a breakthrough curve is formed in nanofiltration processes due to the adsorption of solutes on the membrane at low concentrations. Consequently, rejection is high at the beginning of the process, when adsorption is dominant, and it decreases when all the available sites are occupied. The high rejections found by Peshev et al. mean that, due to the low concentrations considered and the total recirculation operating mode, caffeic acid adsorption was the dominant mechanism. However, in this work, as a result of the higher concentrations considered, as well as the continuous concentration of the feed solution during the process, the adsorption sites became occupied by the solute and its passage through the membrane was favored.

The NF270 membrane also presented similar results, because hydroxytyrosol, tyrosol and caffeic acid showed a passage of almost 100 %, whereas citric acid and hydroxy-stearic acid (as well as larger phenolic compounds) were retained. Furthermore, these results are even more interesting if the permeate flux values are considered. As reported in Figs. 3 and 4, the flux achieved with the NF270 membrane was six times higher than the permeate flux observed with the Dm500 membrane.

As commented in Section 3.2, a good compromise between the rejection of high-molecular weight biophenols and low-molecular-weight biophenols was observed for the NF270 membrane. This high purification capacity as well as the high permeate flux values obtained with this membrane motivated a deeper insight into its performance at different transmembrane pressures. Fig. 6 displays the rejection obtained with this membrane at the TMPs of 15, 25 and 36 bar. The experiment at 36 bar was conducted until a higher concentration level was achieved (VRF of 4.5) to confirm the declining tendency in the

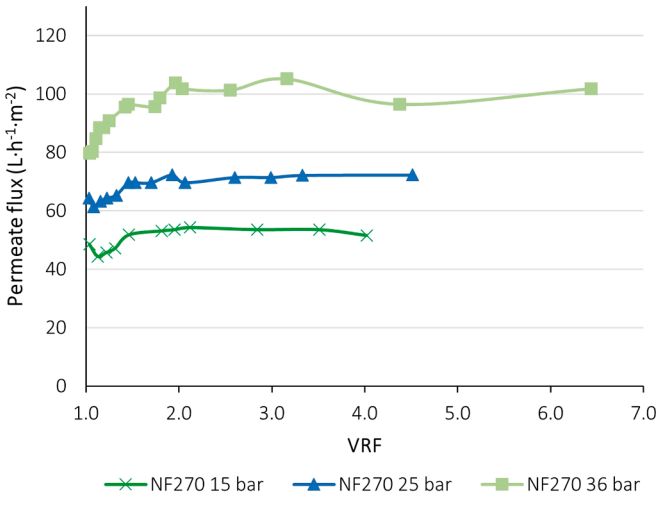

Fig. 4. Values of permeate flux for the NF270 membrane, at the transmembrane pressures of 15 bar, 25 bar and 36 bar.

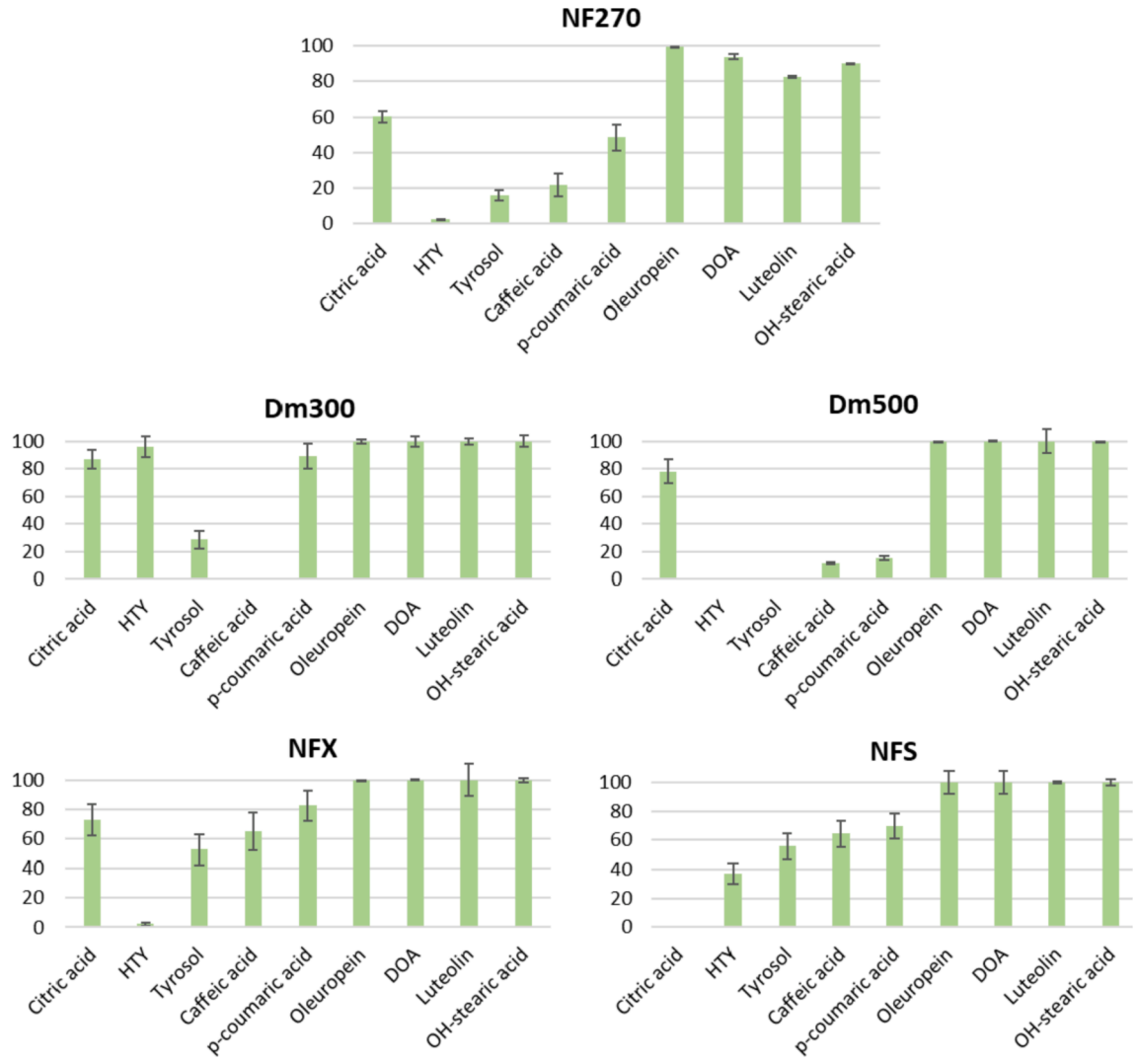

Fig. 5. Rejection values achieved by the different membranes tested, at 36 bar (20 bar for Dm500).

rejection of *p*-coumaric acid, tyrosol and caffeic acid that was observed.

As can be seen in Fig. 6, those compounds which surpassed the membrane MWCO were rejected in high percentages at all pressures. Thus, oleuropein, decarboxymethyl oleuropein aglycone and luteolin displayed high rejection values that were almost constant from the beginning of the OSN process until the highest VRF was achieved.

In contrast to the largest molecules, all the compounds below the MWCO exhibited a clear variation of their rejection with the increase in the VRF and all of them behaved equally. Furthermore, the tendency was drastically different at the lowest pressure applied (15 bar) with respect to the results at 25 and 36 bar.

As many authors have explained, the transport of solutes in nanofiltration processes is not only governed by convection, but also by diffusion across the polymer [23,53,54]. In that case, the initial adsorption of the solutes into the membrane surface is a fundamental stage to promote its interaction with the membrane and, eventually, its permeation. The adsorption phenomenon is also supported by the data discussed in section 3.4. It has been previously described [23,50,51] and it is appreciable in the results at 25 and 36 bar from Fig. 6, that tyrosol, hydroxytyrosol, caffeic acid and *p*-coumaric acid suffered a rapid adsorption on the membrane surface. Accordingly, the rejection values for these compounds were higher at the beginning of the OSN procedure (low VRF), because the highest pressures were responsible for a higher concentration of solutes at the membrane surface, which is consistent with the literature [50]. This situation favoured a rapid occupation of all the saturation sites located on the membrane surface. This fast interaction and adsorption at high pressures occurred until a VRF of 2 was completed. It has been previously demonstrated [50] that, once saturation is completed, convection dominates the transport, while diffusion is not significant. Indeed, these results suggest that, after the adsorption stage, the transport of the compounds was enhanced, then leading to an increase in the permeate concentration and the subsequent decrease in the rejection, as also observed in other works [50–52]. As previously commented, Williams et al. and Imbrogno and Schafer demonstrated that a breakthrough curve is formed in nanofiltration processes when the adsorption of solutes on the membrane occurs at low concentrations [50,51]. Thus, rejection is high at the beginning of the process, when adsorption is dominant, and it decreases when all the available sites are occupied until a steady state is reached. As will be shown in Section 3.4, the interaction of phenolic acids and the membrane surface was higher in comparison with simple phenols. Then, the rejection of caffeic and *p*-coumaric acid did decrease with the VRF, but, at 36 bar, the final value was still higher than the rejection of tyrosol and hydroxytyrosol.

At 36 bar, the importance of the size exclusion process was also notable. As can be seen, the order of less retained compounds was the following: hydroxytyrosol (154 g/mol) and tyrosol (138 g/mol) < caffeic acid (180 g/mol) < p-coumaric acid (164 g/mol) < citric acid (191 g/mol) < luteolin (286 g/mol) < hydroxy-stearic acid (300 g/mol) <

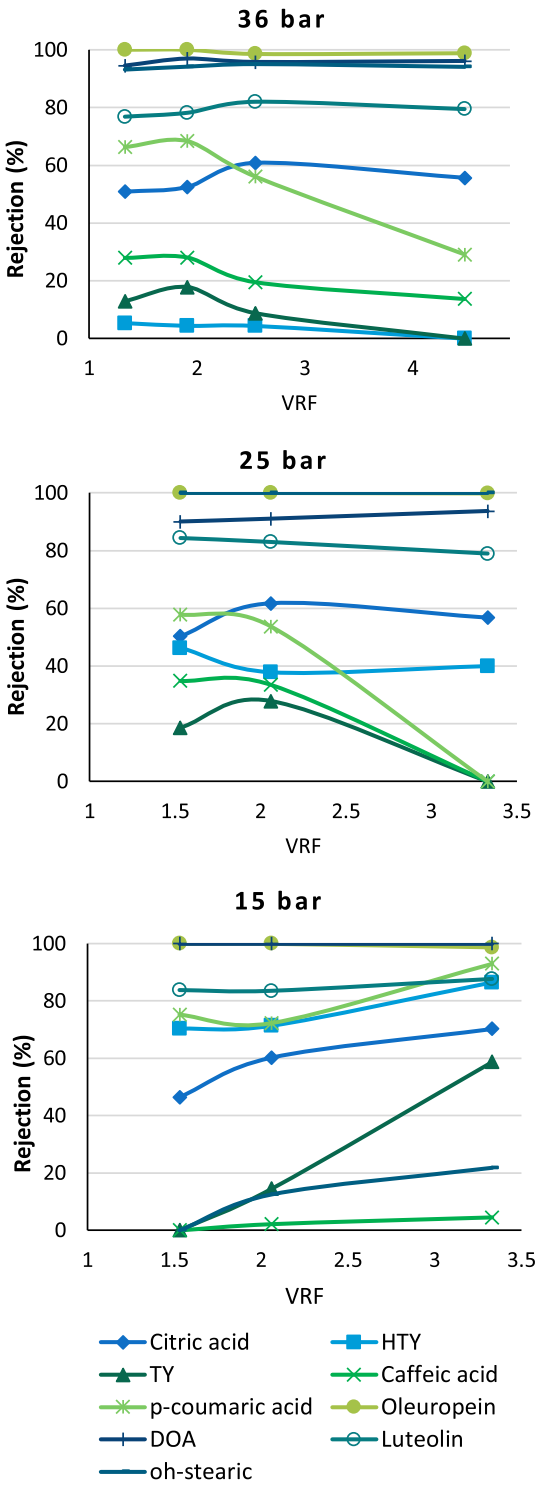

Fig. 6. Evolution of the rejection of each compound from the model solution with the VRF, using the NF270 membrane at 15 bar, 25 bar and 36 bar. The abbreviations of HTY, TY, DOA and OH-stearic acid correspond to hydroxytyrosol, tyrosol, decarboxymethyl oleuropein aglycone and hydroxy stearic acid, respectively. Relative standard deviation between experimental replicates was always below 13 %.

luteolin (286 g/mol) < oleuropein (540 g/mol). This was another indicative of the saturation of the membrane surface, since other authors have reported that steric hindrance becomes more relevant when adsorption stops increasing [23,52,55].

At 25 and 36 bar, which could be considered high pressures, a high concentration polarization was expected during the experiment, then contributing to the transport across the membrane and the decline of the rejection as FRV increased. However, the results obtained at 15 bar (which were obtained after duplicated experiments, as well as all the results from this work) showed a different tendency. In this case, the rejection of the compounds kept increasing during the process, and only those compounds of larger molecular weight displayed a constant rejection. These results could not be explained by a fouling phenomenon, because the permeate flux did not decrease (Fig. 3). Considering that the flux of solvent was almost invariable during the whole experiment, the reduction in the permeate concentration was attributed to the flux of solutes. Possibly, the TMP of 15 bar did not generate the drastic adsorption that was observed for 25 and 36 bar. In contrast, the concentration of compounds at the membrane surface was lower at this lower pressure [50]. Then, it is expected that the interactions with the active layer were not as promoted as at the highest pressures and so they would be more extended in the time. The progressive entrapment of the molecules on the membrane surface could explain the rejection tendency at 15 bar, because the adsorption equilibrium was not observed, and so the diffusion of the compounds towards the permeate side and subsequent desorption in the permeate stream were not fostered.

Additionally, the accumulation of compounds in the retentate (at increasing concentrations) could increase the interactions among them. Some authors have discussed the interactions that can take place between phenolic compounds and other organic molecules [56,57].

In any case, the results obtained at 36 bar were preferred, because the operating conditions permitted a high recovery of low-molecular-weight phenolic compounds, whereas the largest compounds, as well as the sugars (see Section 3.5) were obtained in the retentate.

3.4. Adsorption of compounds onto the surface of the NF270 membrane

As explained above, the NF270 membrane was considered the most promising due to its high efficiency and interesting rejection values. To that end, the possible adsorption of phenolic compounds onto its surface was investigated. In every nanofiltration process, the interaction of the solutes and the membrane is an essential aspect to understand the membrane transport. The compounds are transported not only because of their size (sieving mechanism), but also due to a solution-diffusion mechanism. The initial interaction of the molecules can be a decisive stage for its permeance. However, if the interaction with the membrane surface is too strong, the transport of the compound may be hindered [58], and it could remain bound to the chemical groups of the membrane surface rather than crossing to the permeate side. This phenomenon was investigated here, by evaluating the concentration of the molecules of interest after their contact with the active layer of the membrane. Table 3 shows the adsorption values that were observed after the contact of the conditioned membranes with the model solution (according to Section 2.4).

The simple phenols were poorly adsorbed (hydroxytyrosol) or not adsorbed at all (tyrosol) (Fig. 5). Their low molecular weight as well as

Table 3
Adsorption of the phenolic compounds and organic acids present in the feed solution on the NF270 membrane. Adsorption experiments were conducted during 24 h.

Compound	Adsorption values (mg/m^2)
Citric acid	2.4 ± 0.5
Hydroxytyrosol	0.27 ± 0.04
Tyrosol	–
Caffeic acid	4.7 ± 0.1
p-Coumaric acid	10 ± 1
Oleuropein	8.0 ± 0.1
Decarboxymethyl oleuropein aglycone	–
Luteolin	0.35 ± 0.02
Hydroxy-stearic acid	12.2 ± 0.6

the low contact angle that was observed for the NF270 membrane (indicative of a high hydrophilicity) favored the permeation of these compounds. Regarding the phenolic acids present in the model solution, caffeic acid and *p*-coumaric acid were more adsorbed onto the surface of the NF270 membrane, especially *p*-coumaric acid. This finding contributed to the understanding of the relative rejection of *p*-coumaric acid, which was higher than the rejection of caffeic acid, despite of belonging to the same chemical family and having similar values of molecular weight. In fact, the molecular weight of *p*-coumaric acid (164 g/mol) is lower than the molecular weight of caffeic acid (180 g/mol), which again confirms that other phenomena (not only size-exclusion) influenced their transport across the membrane. Being adsorption a key factor, this molecule could be driven by the solvent throughout the membrane to a larger extent than *p*-coumaric acid, which, in comparison, showed a major affinity for the polymer. Contreras-Jácquez and co-workers also found that phenolic acids (including *p*-coumaric acid) were adsorbed and retained by polyamides in reverse osmosis membranes [59].

For the other compounds (oleuropein, luteolin, decarboxymethyl oleuropein aglycone and hydroxy-stearic acid), the results from Fig. 5 clearly indicate that size exclusion dominated their transport. However, a high contribution of the adsorption process was found for oleuropein and hydroxy-stearic acid. In a number of works, the correlation between solute hydrophobicity and adsorption onto polyamide membranes has been demonstrated [22,59,60]. Thus, the several aromatic rings present in the oleuropein molecule, and the hydrophobic character of the hydroxy-stearic acid favored the hydrophobic interactions with the membrane and explain their large adsorption.

3.5. Separation from sugars

One of the objectives of this work was to identify membranes able to reject the sugars that are normally found in olive-derived waste. Thus, they could be separated from other compounds of high value in order to recover them with high purity. Three carbohydrates were present in the feed solution: sucrose, glucose and fructose. Fig. 7 shows the achieved rejections of these three compounds, after the nanofiltration at 36 bar.

The results reflected in Fig. 7 were highly satisfactory. One of the major challenges for the purification of phenolic compounds from agrofood matrices is the presence of sugars. Many carbohydrates are often coextracted with polyphenols and, usually, sugars are not removed after membrane processes such as ultrafiltration. In fact, whereas polymeric carbohydrates can be rejected by ultrafiltration membranes, monomers and dimers can be easily found in ultrafiltration permeates [17]. Thus, the identification of nanofiltration membranes able to reject the carbohydrates that would be present in these ultrafiltration streams is of high interest.

Taking into account the MWCO of the employed membranes and the molecular weight of sucrose, the observed high rejection is reasonable.

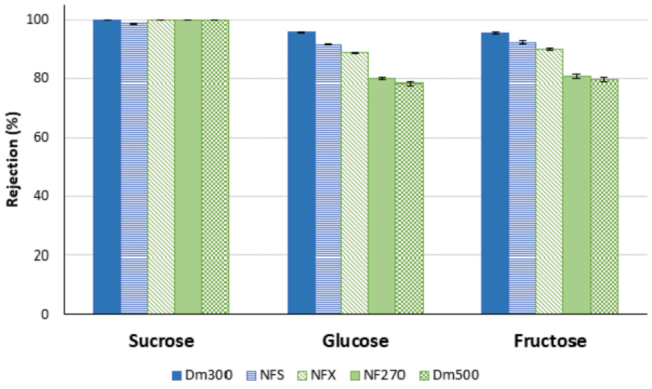

Fig. 7. Rejection of sugars achieved by each membrane at 36 bar.

Furthermore, this performance has been previously reported for the NF270 membrane after an aqueous nanofiltration [17]. The rejection values that were observed for glucose and fructose were very high, considering the molecular weight of these compounds (180 g/mol). Muñoz and co-workers also reported a complete rejection of glucose by the membrane NFX in a hydroalcoholic ambient [61]. Additionally, several authors have described high rejections of glucose and fructose during nanofiltration processes, even when the MWCO of the membranes was far from the molecular weight of the monosaccharides [62,63]. This suggests an additional effect (apart from steric aspects) of the membrane-sugar interactions. As previously commented, Ignacz and Szekely measured the rejection values of 336 different molecules using three commercial DuraMem® polyimide membranes with different MWCO values in methanol [35]. For these membranes the presence of aliphatic rings (not aromatic ones) and hydroxyl groups was observed to improve the rejection, yielding values higher than expected if the molecular weight was only taken into account, while aromatic groups usually negatively affected the rejection value. These results explain the high rejection of sugars observed for the Dm300 and 500 membranes as they present both rings and hydroxyl groups in their structure. The NF270, NFS and NFX membranes have a polyamide active layer, but, from Fig. 7, a similar contribution of these functional groups to an increase in the rejection value can be inferred.

These results demonstrated the feasibility of the tested membranes for purifying the studied polyphenols. Considering the rejection values from Figs. 5 and 7, several membranes allowed the recovery of low-molecular-weight biophenols, which were efficiently separated from other phenolic compounds and from the unwanted sugars present in the wet olive pomace.

3.6. Contact angle

For the most promising membranes in terms of permeate flux and rejections, the contact angle was determined (Table 4). For the virgin membranes, their water contact angle was retrieved from the literature, whereas it was experimentally determined for the conditioned membranes (after immersion in ethanol/water 50:50 (v/v)) and after the nanofiltration of the simulated wet olive pomace extract. Additionally, the contact angle of a droplet of ethanol/water 50:50 (v/v) was determined.

The water contact angle of the pristine membranes allowed the evaluation of the polarity of the polymers. A higher value of the contact

Table 4
Water contact angle and ethanol/water 50:50 (v/v) contact angle for the NF270, Dm300, Dm500, NFX and NFS membranes. The values for the pristine membrane, the membrane after the conditioning and the membrane after the nanofiltration process are reported.

Membrane	Water contact angle			Ethanol 50 % (v/v) contact angle
	Native	After immersion in working solvent	After nanofiltration	After immersion in working solvent
NF270	15.9 ± 1.3° [34]	33.5 ± 0.6°	64 ± 5°	[d]
Dm300[a]	59° [31][c]	69 ± 2°	59 ± 5°	12 ± 4°
Dm500[b]	67.1 ± 0.8° [65]	76 ± 1°	64 ± 4°	36 ± 4°
NFS	49.79° [36][c]	26 ± 2°	–	19 ± 3°
NFX	17.6 ± 2.8° [66]	24 ± 2°	–	11 ± 3°

[a] Dm300: DuraMem®300.
[b] Dm500: DuraMem®500.
[c] Measured deviation was not reported.
[d] Measurement was not possible due to the very small contact angle of the solvent drop.

angle indicated a lower hydrophilicity [36,67,68], which was observed for the Dm300 and Dm500 membranes. This was in line with their material (modified polyimide). The rest of the membranes were based on polyamide polymers and were considered more hydrophilic.

In order to assess the relation of the polarity of the membrane active layer and the observed permeate flux, the water contact angle and the ethanol/water 50:50 (v/v) contact angle of the conditioned membranes was studied. This was considered to be more reliable, because the utilization of the membrane was performed after its overnight immersion in the working solvent. Van der Bruggen et al. demonstrated that the polarity of organic membranes can be modified after their contact with organic solvents such as ethanol [38]. Then, this strategy allowed the evaluation of the real hydrophilic or hydrophobic character of the membranes, right before the OSN process. As can be seen in Table 4, a general increase in the water contact angle was observed, prompted by the presence of ethanol in the solvent mixture, except in the case of the NFS membrane, as its water contact angle decreased after immersion in the working solvent (some insights about the contact angle of the NFS membrane have been provided in Section 3.3). Still, the Dm300 and Dm500 membranes continued to be the least hydrophilic membranes, which was in line with their values of permeate flux. As summarized in Figs. 3 and 4, the DuraMem® membranes displayed the lowest flux, both in the case of the nanofiltration of the pure solvent and model solution.

Regarding the rest of the membranes, their water contact angle reached a value between 24º and 34°. Despite of their close polarity, a large difference between their values of permeate flux was found. This can be explained by the MWCO, which was higher for the NF270 membrane. Zyłła and co-workers also described that the NF270 membrane stood out with respect to NFX and other polymeric membranes in terms of permeate flux, despite close values of the contact angle [66].

The ethanol/water 50:50 (v/v) contact angle of the conditioned membranes was also evaluated. In the case of the NF270 membrane, the solvent droplet was almost immediately dispersed throughout the active layer, hindering the evaluation of the contact angle. The quick filtration of the solvent indicated a high affinity between this membrane and the ethanol/water 50:50 (v/v). This was already suggested by the results related to the permeate flux presented in Section 3.2. For the rest of membranes, the droplet was stable enough to perform the measurement. In general, the observed values were lower than the reported water contact angle for each membrane. This was expected, as the DuraMem® membranes and the NFS and NFX membranes are specific for organic solvents. Then, a higher affinity for ethanol/water 50:50 (v/v) than for water is reasonable. Furthermore, it should also be noted that the superficial tension of the solvent is lower than the superficial tension of water, then contributing to the immediate filtration of the solvent droplet throughout the membrane surface [69]. These results are consistent with the values of permeate flux (Fig. 3A) reported for each membrane. The membrane with the highest permeate flux (NF270) displayed the lowest solvent contact angle, followed by the NFX and NFS membranes, which comprised the second group in terms of permeate flux. Finally, the lowest permeate flux was observed DuraMem® membranes, as well as the highest values of ethanol/water 50:50 (v/v) contact angle.

After the nanofiltration of the hydroalcoholic model solution (containing phenolic compounds, organic and fatty acids and sugars) the water contact angle for all the membranes became much closer, in the range of 59–64°. This was another indicative of the adsorption of compounds onto the membrane, as discussed in section 3.3. Sotto et al. also reported an adsorbed layer on the membrane surface formed after solutes adsorption [23]. In the case of the current study, this layer always led to an increase of the hydrophobicity of the membranes, independently of their initial polarity. In the case of the DuraMem® membranes, this modulation of the active layer was less notable, as those polymers were already highly hydrophobic prior to their contact with the solvent.

3.7. Atomic force microscopy characterization

The effect of the working solvent on the active layer of the tested membranes was investigated by AFM. This allowed studying possible modifications of the surface structure.

The height images in Fig. 8A show that the polymers corresponding to all membranes display a nodular structure. This is in line with previous works reporting a microscopy-based characterization of nanofiltration membranes [72–74]. The membrane pores correspond to the interstitial space between the polymer fibers, which can be packed in nodules or not. A complementary image to those in column A is given in column B. The adhesion signal reflects the different interaction forces that are established between the membrane material and the AFM probe [75]. Those forces were stronger when the probe approached a nodule, and they were less relevant when the probe went over the pores. In consequence, the images in Fig. 8B correspond to the flip side of the height images, as in a picture negative. The holes observed in Fig. 8B are complementary to the nodules in Fig. 8A and the space among the nodules, correspond to the protrusions reflected in Fig. 8B. By studying these images, both in the native and conditioned state of the membranes, interesting conclusions can be reached regarding the modification of the polymer structure.

The NF270 membrane exhibited well-defined nodules in its native form (Fig. 8A and 8B). According to Boo et al., the pore size of the native membrane is near 0.8 nm [76]. After its immersion in ethanol/water 50:50 (v/v), a drastic change can be observed on its surface. Zhang et al., observed similar results with a polyamide membrane and explained this variation by the hydrolysis of the polyamide chains, prompted by the solvent [77].

The nodules present in the height images of the DuraMem® membranes (Dm300 and Dm500) were smaller than those in the NF270 membrane. This suggests a smaller pore size, as thinner fibers generate smaller holes among them. By observing the height and adhesion images it is possible to detect a slight thickening of the nodules of both membranes, which can be attributed to a swelling phenomenon. However, the effect of the solvent was not so relevant for these membranes, thus suggesting a more stable structure of the active layer. This stability was expected, as the DuraMem® membranes are recommended for their use with organic solvents.

The Synder membranes (NFX and NFS) presented large nodules (Fig. 8A), similarly to the NF270, which also contains polyamide in its active layer. The nodules from the NFX and NFS were thick and highly packed. As reflected by the adhesion signal (Fig. 8B), the valleys were less marked in these membranes. The effect of the membrane immersion in ethanol/water 50:50 (v/v) was highly intense, as in the case of the NF270 membrane. The diameter of the nodules was drastically reduced, leading to a granular structure, reflecting fiber aggregates (Fig. 8C).

Interestingly, all membranes displayed a similar topology after their conditioning, as it is shown in Fig. 8D. Due to the effect of the solvent, the polymer suffer a reorganization that resulted in the substitution of the nodular structure by a spongier structure. This has been related to the clustering of hydrophilic and hydrophobic groups from the membrane surface [70,78,79].

4. Conclusions

Several OSN membranes have been studied for the recovery of phenolic compounds from a hydroalcoholic extract of wet olive pomace. Some of the tested membranes, such as oNF-1, oNF-2 and DuraMem® 150, produced extremely low values of permeate flux, because of a poor interaction between the active layer and the solvent molecules. On the contrary, the Dm300, Dm500, NFX, NFS and NF270 membranes displayed acceptable flux. The NF270 membrane stood out due to high values of permeate flux, near 100 $L \cdot h^{-1} \cdot m^2$. Regarding the rejection values, the selected membranes permitted the fractionation of the phenolic compounds, as well as their purification, within the same OSN

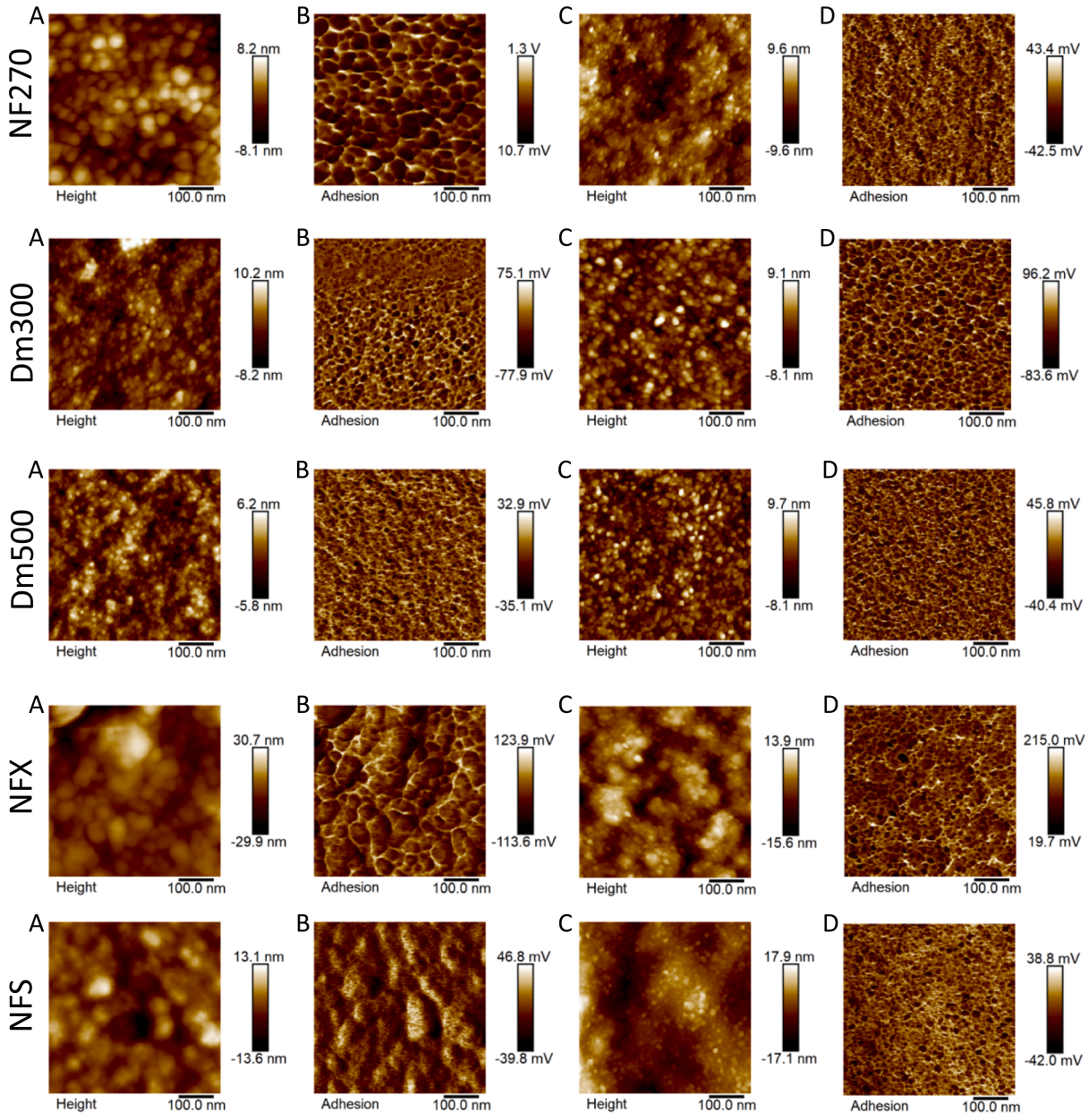

Fig. 8. AFM characterization of the tested membranes. A and B images correspond to the native membranes, monitoring the height (A) and the adhesion signal (B). C and D images correspond to the conditioned membrane with ethanol/water 50:50 (v/v), monitoring the height (C) and adhesion signal (D).

procedure. Thus, the compounds of interest were recovered in the permeate, whereas some unwanted compounds such as the sugars, free fatty acids and organic acids were rejected. These results suggest that a hydrophilic membrane, with an active layer based on cross-linked polyamide (as in the case of the NF270 or NFX membrane) can be effective to recover phenolic compounds from the wet olive pomace, after a hydroalcoholic extraction. Furthermore, a MWCO of 300–400 Da allowed the fractionation of the biophenols, achieving the separation the high-molecular-weight polyphenols from those of low-molecular-weight, which are highly valuable.

The optimization of membrane processes in the presence of organic solvents permits the utilization of these organic solvents in previous stages, such as solid–liquid extraction. This lead, in most cases, to higher efficiency in terms of recovery of bioactive compounds than the utilization of water as solvent. The results presented here indicate that OSN is an effective strategy for obtaining highly pure phenolic compounds from vegetable residues such as wet olive pomace. This generates a source of income from an environmentally concerning by-product and contributes to recycle it.

CRediT authorship contribution statement

Carmen M. Sánchez-Arévalo: Validation, Investigation, Writing – original draft, Writing – review & editing, Visualization. **Tim Croes:** Validation. **Bart Van der Bruggen:** Conceptualization, Validation, Resources, Writing – original draft, Writing – review & editing, Supervision, Project administration, Funding acquisition. **María Cinta Vincent-Vela:** Conceptualization, Validation, Writing – original draft, Writing – review & editing, Supervision, Project administration, Funding acquisition. **Silvia Álvarez-Blanco:** Conceptualization, Validation, Writing – original draft, Writing – review & editing, Supervision, Project administration, Funding acquisition.

Declaration of Competing Interest

The authors declare that they have no known competing financial interests or personal relationships that could have appeared to influence the work reported in this paper.

Data availability

Data will be made available on request.

Acknowledgements

The authors would like to thank Laura Teruel Biosca for her technical support. Additionally, Electron Microscopy Service of the Polytechnic University of Valencia is gratefully acknowledged for help with AFM characterization.

Funding.

The grant CTM2017-88645-R was funded by MCIN/AEI/ 10.13039/501100011033 and by ERDF A way of making Europe. Additionally, the grant PRE2018-08524 was funded by MCIN/AEI/ 10.13039/501100011033 and by ESF Investing in your future.

Appendix A. Supplementary material

Supplementary data to this article can be found online at https://doi.org/10.1016/j.seppur.2022.122396.

References

[1] V. Sygouni, A.G. Pantziaros, I.C. Iakovides, E. Sfetsa, P.I. Bogdou, E. A. Christoforou, C.A. Paraskeva, Treatment of two-phase olive mill wastewater and recovery of phenolic compounds using membrane technology, Membranes (Basel). 9 (2019) 27, https://doi.org/10.3390/membranes9020027.

[2] E. Roselló-Soto, M. Koubaa, A. Moubarik, R.P. Lopes, J.A. Saraiva, N. Boussetta, N. Grimi, F.J. Barba, Emerging opportunities for the effective valorization of wastes and by-products generated during olive oil production process: non-conventional methods for the recovery of high-added value compounds, Trends Food Sci. Technol. 45 (2015) 296–310, https://doi.org/10.1016/j.tifs.2015.07.003.

[3] P. Tapia-Quirós, M.F. Montenegro-Landívar, M. Reig, X. Vecino, T. Alvarino, J. L. Cortina, J. Saurina, M. Granados, Olive mill and winery wastes as viable sources of bioactive compounds: a study on polyphenols recovery, Antioxidants. 9 (2020) 1–15, https://doi.org/10.3390/antiox9111074.

[4] O.C. Adebooye, A.M. Alashi, R.E. Aluko, A brief review on emerging trends in global polyphenol research, J. Food Biochem. 42 (2018) 1–7, https://doi.org/10.1111/jfbc.12519.

[5] V. Sant'Anna, A. Brandelli, L.D.F. Marczak, I.C. Tessaro, Kinetic modeling of total polyphenol extraction from grape marc and characterization of the extracts, Sep. Purif. Technol. 100 (2012) 82–87.

[6] T.W. Caldas, K.E.L. Mazza, A.S.C. Teles, G.N. Mattos, A.I.S. Brígida, C.A. Conte-Junior, R.G. Borguini, R.L.O. Godoy, L.M.C. Cabral, R.V. Tonon, Phenolic compounds recovery from grape skin using conventional and non-conventional extraction methods, Ind. Crops Prod. 111 (2018) 86–91, https://doi.org/10.1016/j.indcrop.2017.10.012.

[7] C.M. Sánchez-Arévalo, M.C. Vincent-Vela, S. Álvarez-Blanco, Revalorization of two-phase olive mill wastewater: Recovery of antioxidant, bioactive compounds from a phytotoxic residue, in: Int. Conf. Water Sustain., Barcelona, 2021, pp. 32–33.

[8] C.M. Sánchez-Arévalo, H. Ellicott, M.-C. Vincent-Vela, S. Álvarez-Blanco, Assesment of several organic and inorganic membranes to ultrafilter a phenolic extract from two-phase olive mill wastewater, in: II Int. Congr. Water Sustain., Barcelona, 2021.

[9] R. Shukla, M. Cheryan, Stability and performance of ultrafiltration membranes in aqueous ethanol, Sep. Sci. Technol. 38 (2003) 1533–1547, https://doi.org/10.1081/SS-120019091.

[10] P. Marchetti, M.F. Jimenez Solomon, G. Szekely, A.G. Livingston, Molecular separation with organic solvent nanofiltration: a critical review, Chem. Rev. 114 (2014) 10735–10806, https://doi.org/10.1021/CR500006J.

[11] A.M. Tandel, W. Guo, K. Bye, L. Huang, M. Galizia, H. Lin, Designing organic solvent separation membranes: polymers, porous structures, 2D materials, and their combinations, Mater. Adv. 2 (2021) 4574–4603, https://doi.org/10.1039/d1ma00373a.

[12] R. Shevate, D.L. Shaffer, Large-area 2D covalent organic framework membranes with tunable single-digit nanopores for predictable mass transport, ACS Nano 16 (2022) 2407–2418, https://doi.org/10.1021/acsnano.1c08804.

[13] X.Y. Gong, Z.H. Huang, H. Zhang, W.L. Liu, X.H. Ma, Z.L. Xu, C.Y. Tang, Novel high-flux positively charged composite membrane incorporating titanium-based MOFs for heavy metal removal, Chem. Eng. J. 398 (2020) 125706, https://doi.org/10.1016/J.CEJ.2020.125706.

[14] J. Campbell, J.D.S. Burgal, G. Szekely, R.P. Davies, D.C. Braddock, A. Livingston, Hybrid polymer/MOF membranes for Organic Solvent Nanofiltration (OSN): chemical modification and the quest for perfection, J. Memb. Sci. 503 (2016) 166–176, https://doi.org/10.1016/J.MEMSCI.2016.01.024.

[15] U. Beuscher, E.J. Kappert, J.G. Wijmans, Membrane research beyond materials science, J. Memb. Sci. 643 (2022) 119902, https://doi.org/10.1016/J.MEMSCI.2021.119902.

[16] B. Díaz-Reinoso, A. Moure, H. Domínguez, J.C. Parajó, Ultra- and nanofiltration of aqueous extracts from distilled fermented grape pomace, J. Food Eng. 91 (2009) 587–593, https://doi.org/10.1016/j.jfoodeng.2008.10.007.

[17] C.M. Sánchez-Arévalo, Á. Jimeno-Jiménez, C. Carbonell-Alcaina, M.C. Vincent-Vela, S. Álvarez-Blanco, Effect of the operating conditions on a nanofiltration process to separate low-molecular-weight phenolic compounds from the sugars present in olive mill wastewaters, Process Saf. Environ. Prot. 148 (2021) 428–436, https://doi.org/10.1016/j.psep.2020.10.002.

[18] A. Alfano, L. Corsuto, R. Finamore, M. Savarese, F. Ferrara, S. Falco, G. Santabarbara, M. De Rosa, C. Schiraldi, Valorization of olive mill wastewater by membrane processes to recover natural antioxidant compounds for cosmeceutical and nutraceutical applications or functional foods, Antioxidants. 7 (6) (2018) 72, https://doi.org/10.3390/antiox7060072.

[19] A. Jiménez, R. Rodríguez, I. Fernández-Caro, R. Guillén, J. Fernández-Bolaños, A. Heredia, Olive fruit cell wall: degradation of cellulosic and hemicellulosic polysaccharides during ripening, J. Agric. Food Chem. 49 (2001) 2008–2013, https://doi.org/10.1021/jf000809v.

[20] J. Yu, K. Wang, D.M. Beckles, Starch branching enzymes as putative determinants of postharvest quality in horticultural crops, BMC Plant Biol. 21 (1) (2021), https://doi.org/10.1186/s12870-021-03253-6.

[21] C. Ghilardi, P. Sanmartin Negrete, A.A. Carelli, V. Borroni, Evaluation of olive mill waste as substrate for carotenoid production by Rhodotorula mucilaginosa, Bioresour. Bioprocess. 7 (2020) 1–11, https://doi.org/10.1186/s40643-020-00341-7.

[22] J.M. Arsuaga, M.J. López-Muñoz, A. Sotto, Correlation between retention and adsorption of phenolic compounds in nanofiltration membranes, Desalination. 250 (2010) 829–832, https://doi.org/10.1016/j.desal.2008.11.051.

[23] A. Sotto, J.M. Arsuaga, B. Van der Bruggen, Sorption of phenolic compounds on NF/RO membrane surfaces: influence on membrane performance, Desalination. 309 (2013) 64–73, https://doi.org/10.1016/j.desal.2012.09.023.

[24] M. Cifuentes-Cabezas, C. Carbonell-Alcaina, M.C. Vincent-Vela, J.A. Mendoza-Roca, S. Álvarez-Blanco, Comparison of different ultrafiltration membranes as first step for the recovery of phenolic compounds from olive-oil washing wastewater, Process Saf. Environ. Prot. 149 (2021) 724–734, https://doi.org/10.1016/j.psep.2021.03.035.

[25] C.M. Sánchez-Arévalo, A. Iborra-Clar, M.C. Vincent-Vela, S. Álvarez-Blanco, Exploring the extraction of the bioactive content from the two-phase olive mill waste and further purification by ultrafiltration, LWT. 165 (2022) 113742, https://doi.org/10.1016/j.lwt.2022.113742.

[26] R. Dreywood, Qualitative test for carbohydrate material, Ind. Eng. Chem. - Anal. Ed. 18 (8) (1946) 499.

[27] T.G. Ludwig, H.J.V. Goldberg, The Anthrone method for the determination of carbohydrates in foods and in oral rinsing, J. Dent. Res. 35 (1956) 90–94, https://doi.org/10.1177/00220345560350012301.

[28] S. Zeidler, U. Kätzel, P. Kreis, Systematic investigation on the influence of solutes on the separation behavior of a PDMS membrane in organic solvent nanofiltration, J. Memb. Sci. 429 (2013) 295–303, https://doi.org/10.1016/J.MEMSCI.2012.11.056.

[29] D. Peshev, L.G. Peeva, G. Peev, I.I.R. Baptista, A.T. Boam, Application of organic solvent nanofiltration for concentration of antioxidant extracts of rosemary (Rosmarinus officiallis L.), Chem. Eng. Res. Des. 89 (2011) 318–327, https://doi.org/10.1016/j.cherd.2010.07.002.

[30] B. Tylkowski, I. Tsibranska, R. Kochanov, G. Peev, M. Giamberini, Concentration of biologically active compounds extracted from Sideritis ssp. L. by nanofiltration, Food Bioprod. Process. 89 (2011) 307–314, https://doi.org/10.1016/j.fbp.2010.11.003.

[31] M. Razali, C. Didaskalou, J.F. Kim, M. Babaei, E. Drioli, Y.M. Lee, G. Szekely, Exploring and exploiting the effect of solvent treatment in membrane separations, ACS Appl. Mater. Interfaces. 9 (2017) 11279–11289, https://doi.org/10.1021/acsami.7b01879.

[32] S. Blumenschein, Application of Organic Solvent Nanofiltration for Multi-Purpose Production, Tecnical University of Dortmund, 2017.

[33] K. Grundke, S. Michel, G. Knispel, A. Grundler, Wettability of silicone and polyether impression materials: characterization by surface tension and contact angle measurements, Colloids Surf. A Physicochem. Eng. Asp. 317 (2008) 598–609, https://doi.org/10.1016/J.COLSURFA.2007.11.046.

[34] G.S. Vieira, F.K.V. Moreira, R.L.S. Matsumoto, M. Michelon, F.M. Filho, M. D. Hubinger, Influence of nanofiltration membrane features on enrichment of jussara ethanolic extract (Euterpe edulis) in anthocyanins, J. Food Eng. 226 (2018) 31–41, https://doi.org/10.1016/J.JFOODENG.2018.01.013.

[35] G. Ignacz, G. Szekely, Deep learning meets quantitative structure–activity relationship (QSAR) for leveraging structure-based prediction of solute rejection in organic solvent nanofiltration, J. Memb. Sci. 646 (2022) 120268, https://doi.org/10.1016/J.MEMSCI.2022.120268.

[36] S. Jafarinejad, H. Park, H. Mayton, S.L. Walker, S.C. Jiang, Concentrating ammonium in wastewater by forward osmosis using a surface modified

nanofiltration membrane, Environ. Sci. Water Res. Technol. 5 (2019) 246–255, https://doi.org/10.1039/C8EW00690C.
[37] A. Premachandra, S. O'Brien, N. Perna, J. McGivern, R. LaRue, D.R. Latulippe, Treatment of complex multi-sourced industrial wastewater — new opportunities for nanofiltration membranes, Chem. Eng. Res. Des. 168 (2021) 499–509, https://doi.org/10.1016/j.cherd.2021.01.005.
[38] B. Van der Bruggen, J. Geens, C. Vandecasteele, Influence of organic solvents on the performance of polymeric nanofiltration membranes, Sep. Sci. Technol. 37 (2002) 783–797, https://doi.org/10.1081/SS-120002217.
[39] J.R.M. de Melo, J. Tres, J. Steffens, M. Vladimir Oliveira, Di LuccioDesolventizing organic solvent-soybean oil miscella using ultrafiltration ceramic membranes, J. Memb. Sci. 475 (2015) 357–366, https://doi.org/10.1016/j.memsci.2014.10.029.
[40] I.S. Argyle, A. Pihlajamäki, M.R. Bird, Black tea liquor ultrafiltration: effect of ethanol pre-treatment upon fouling and cleaning characteristics, Food Bioprod. Process. 93 (2015) 289–297, https://doi.org/10.1016/j.fbp.2014.10.010.
[41] A. García, S. Álvarez, F. Riera, R. Álvarez, J. Coca, Water and hexane permeate flux through organic and ceramic membranes: Effect of pre-treatment on hexane permeate flux, J. Memb. Sci. 253 (2005) 139–147, https://doi.org/10.1016/j.memsci.2004.11.030.
[42] M. Mänttäri, A. Pihlajamäki, M. Nyström, Effect of pH on hydrophilicity and charge and their effect on the filtration efficiency of NF membranes at different pH, J. Memb. Sci. 280 (2006) 311–320, https://doi.org/10.1016/j.memsci.2006.01.034.
[43] L.D. Nghiem, A.I. Schäfer, M. Elimelech, Pharmaceutical retention mechanisms by nanofiltration membranes, Environ. Sci. Technol. 39 (2005) 7698–7705, https://doi.org/10.1021/es0507665.
[44] A. Böcking, Membrane Transport Properties and Process Design in Nanofiltration with Organic Solvents and Aqueous Solvent Mixtures, Aachen University, 2020.
[45] T. Roncal, L. Lorenzo, S. Prieto-Fernández, J.R. Ochoa-Gómez, Purification and concentration of formic acid from formic acid/gluconic acid mixtures by two successive steps of nanofiltration and reactive liquid-liquid extraction, Sep. Purif. Technol. 286 (2022) 120492.
[46] Y. Kiso, Y. Sugiura, T. Kitao, K. Nishimura, Effects of hydrophobicity and molecular size on rejection of aromatic pesticides with nanofiltration membranes, J. Memb. Sci. 192 (2001) 1–10, https://doi.org/10.1016/S0376-7388(01)00411-2.
[47] Y. Thiermeyer, S. Blumenschein, M. Skiborowski, Fundamental insights into the rejection behavior of polyimide-based OSN membranes, Sep. Purif. Technol. 265 (2021) 118492, https://doi.org/10.1016/J.SEPPUR.2021.118492.
[48] L. Wu, Y. Xu, Z. Yang, Q. Feng, Hydroxytyrosol and olive leaf extract exert cardioprotective effects by inhibiting GRP78 and CHOP expression, J. Biomed. Res. 32 (2018) 371–379, https://doi.org/10.7555/JBR.32.20170111.
[49] Z. Zhao, T. Sun, Y. Jiang, L. Wu, X. Cai, X. Sun, X. Sun, Photooxidative damage in retinal pigment epithelial cells via GRP78 and the protective role of grape skin polyphenols, Food Chem. Toxicol. 74 (2014) 216–224, https://doi.org/10.1016/J.FCT.2014.10.001.
[50] A. Imbrogno, A.I. Schäfer, Micropollutants breakthrough curve phenomena in nanofiltration: impact of operational parameters, Sep. Purif. Technol. 267 (2021) 1–13, https://doi.org/10.1016/j.seppur.2021.118406.
[51] M.E. Williams, J.A. Hestekin, C.N. Smothers, D. Bhattacharyya, Separation of organic pollutants by reverse osmosis and nanofiltration membranes: mathematical models and experimental verification, Ind. Eng. Chem. Res. 38 (1999) 3683–3695, https://doi.org/10.1021/IE990140L.
[52] L.D. Nghiem, A.I. Schäfer, M. Elimelech, Removal of natural hormones by nanofiltration membranes: measurement, modeling, and mechanisms, Environ. Sci. Technol. 38 (2004) 1888–1896, https://doi.org/10.1021/ES034952R.
[53] S. Darvishmanesh, J. Degrève, B. Van der Bruggen, Comparison of pressure driven transport of ethanol/n-hexane mixtures through dense and microporous membranes, Chem. Eng. Sci. 64 (2009) 3914–3927, https://doi.org/10.1016/j.ces.2009.05.032.
[54] A.J.C. Semião, M. Foucher, A.I. Schäfer, Removal of adsorbing estrogenic micropollutants by nanofiltration membranes: Part B—Model development, J. Memb. Sci. 431 (2013) 257–266, https://doi.org/10.1016/j.memsci.2012.11.079.
[55] E.A. McCallum, H. Hyung, T.A. Do, C.H. Huang, J.H. Kim, Adsorption, desorption, and steady-state removal of 17β-estradiol by nanofiltration membranes, J. Memb. Sci. 319 (2008) 38–43, https://doi.org/10.1016/J.MEMSCI.2008.03.014.
[56] A. Giacobbo, A. Moura Bernardes, M. Filipe Rosa, M. de Pinho, Concentration polarization in ultrafiltration/nanofiltration for the recovery of polyphenols from winery wastewaters, Membranes (Basel). 8 (3) (2018) 46.
[57] C.M. Galanakis, E. Markouli, V. Gekas, Recovery and fractionation of different phenolic classes from winery sludge using ultrafiltration, Sep. Purif. Technol. 107 (2013) 245–251, https://doi.org/10.1016/J.SEPPUR.2013.01.034.
[58] H. Xu, K. Xiao, X. Wang, S. Liang, C. Wei, X. Wen, X. Huang, Outlining the roles of membrane-Foulant and Foulant-Foulant interactions in organic fouling during microfiltration and ultrafiltration: a mini-review, Front. Chem. 8 (2020) 417, https://doi.org/10.3389/FCHEM.2020.00417/BIBTEX.
[59] V. Contreras-Jácquez, U. Valenzuela-Vázquez, D.A. Grajales-Hernández, J. C. Mateos-Díaz, M. Arrellano-Plaza, M.E. Jara-Marini, A. Asaff-Torres, Pilot-scale integrated membrane system for the separation and concentration of compounds of industrial interest from tortilla industry wastewater (Nejayote), Waste Biomass Valor. 13 (2022) 345–360, https://doi.org/10.1007/s12649-021-01530-x.
[60] L. Braeken, R. Ramaekers, Y. Zhang, G. Maes, B. Van Der Bruggen, C. Vandecasteele, Influence of hydrophobicity on retention in nanofiltration of aqueous solutions containing organic compounds, J. Memb. Sci. 252 (2005) 195–203, https://doi.org/10.1016/J.MEMSCI.2004.12.017.
[61] P. Muñoz, K. Pérez, A. Cassano, R. Ruby-Figueroa, Recovery of anthocyanins and monosaccharides from grape marc extract by nanofiltration membranes, Molecules. 26 (2021) 1–12, https://doi.org/10.3390/molecules26072003.
[62] J.A.A. Mejia, A. Ricci, A.S. Figueiredo, A. Versari, A. Cassano, M.N. de Pinho, G. P. Parpinello, Membrane-based operations for the fractionation of polyphenols and polysaccharides from winery sludges, Food Bioprocess Technol. 15 (2022) 933–948, https://doi.org/10.1007/s11947-022-02795-3.
[63] S. Yammine, R. Rabagliato, X. Vitrac, M.M. Peuchot, R. Ghidossi, The use of nanofiltration membranes for the fractionation of polyphenols from grape pomace extracts, OENO One. 53 (2019) 11–26, https://doi.org/10.20870/OENO-ONE.2019.53.1.2342.
[65] U.T. Syed, C. Brazinha, J.G. Crespo, J.M. Ricardo-da-Silva, Valorisation of grape pomace: fractionation of bioactive flavan-3-ols by membrane processing, Sep. Purif. Technol. 172 (2017) 404–414, https://doi.org/10.1016/j.seppur.2016.07.039.
[66] R. Zyłła, M. Foszpanczyk, I. Kaminska, M. Kudzin, J. Balcerzak, S. Ledakowicz, Impact of polymer membrane properties on the removal of pharmaceuticals, Membranes (Basel). 12 (2022), https://doi.org/10.3390/membranes12020150.
[67] K.Y. Law, Definitions for hydrophilicity, hydrophobicity, and superhydrophobicity: getting the basics right, J. Phys. Chem. Lett. 5 (2014) 686–688, https://doi.org/10.1021/jz402762h.
[68] Y. Kaya, H. Barlas, S. Arayici, Nanofiltration of Cleaning-in-Place (CIP) wastewater in a detergent plant: effects of pH, temperature and transmembrane pressure on flux behavior, Sep. Purif. Technol. 65 (2009) 117–129, https://doi.org/10.1016/J.SEPPUR.2008.10.034.
[69] M. Sharma, P.K. Roy, J. Barman, K. Khare, Mobility of aqueous and binary mixture drops on lubricating fluid-coated slippery surfaces, Langmuir. 35 (2019) 7672–7679, https://doi.org/10.1021/ACS.LANGMUIR.9B00483/SUPPL_FILE/LA9B00483_SI_005.AVI.
[70] S.B. Sigurdardóttir, M.S.M. Sueb, M. Pinelo, Membrane compaction, internal fouling, and membrane preconditioning as major factors affecting performance of solvent resistant nanofiltration membranes in methanol solutions, Sep. Purif. Technol. 227 (2019) 1–8, https://doi.org/10.1016/j.seppur.2019.115686.
[72] V. Freger, Swelling and morphology of the skin layer of polyamide composite membranes: an atomic force microscopy study, Environ. Sci. Technol. 38 (2004) 3168–3175, https://doi.org/10.1021/es034815u.
[73] X. Lu, S. Nejati, Y. Choo, C.O. Osuji, J. Ma, M. Elimelech, Elements provide a clue: nanoscale characterization of thin-film composite polyamide membranes, ACS Appl. Mater. Interfaces. 7 (2015) 16917–16922, https://doi.org/10.1021/acsami.5b05478.
[74] J.J. Torres, N.E. Rodriguez, J. Toledo Arana, N. Ochoa, J. Ariel, C.P. Marchese, Ultrafiltration polymeric membranes for the purification of biodiesel from ethanol, J. Clean. Prod. 141 (2017) 641–647, https://doi.org/10.1016/j.jclepro.2016.09.130.
[75] J. Llanos, P.M. Williams, S. Cheng, D. Rogers, C. Wright, Á. Pérez, P. Cañizares, Characterization of a ceramic ultrafiltration membrane in different operational states after its use in a heavy-metal ion removal process, Water Res. 44 (2010) 3522–3530, https://doi.org/10.1016/j.watres.2010.03.036.
[76] C. Boo, Y. Wang, I. Zucker, Y. Choo, C.O. Osuji, M. Elimelech, High performance nanofiltration membrane for effective removal of perfluoroalkyl substances at high water recovery, Environ. Sci. Technol. 52 (2018) 7279–7288, https://doi.org/10.1021/acs.est.8b01040.
[77] R. Zhang, S. Su, S. Gao, J. Tian, Reconstruction of the polyamide film in nanofiltration membranes via the post-treatment with a ternary mixture of ethanol-water-NaOH: Mechanism and effect, Desalination. 519 (2021) 115317.
[78] J. Geens, B. Van der Bruggen, C. Vandecasteele, Characterisation of the solvent stability of polymeric nanofiltration membranes by measurement of contact angles and swelling, Chem. Eng. Sci. 59 (2004) 1161–1164, https://doi.org/10.1016/J.CES.2004.01.003.
[79] B. Van der Bruggen, J. Geens, C. Vandecasteele, Fluxes and rejections for nanofiltration with solvent stable polymeric membranes in water, ethanol and n-hexane, Chem. Eng. Sci. 57 (2002) 2511–2518, https://doi.org/10.1016/S0009-2509(02)00125-2.